CORROSION SCIENCE AND TECHNOLOGY, Vol.2, No.5(2003), pp.225~232

Spalling of the Oxide Scales Foemed on Stainless Steels During Cooling

Isao Saeki, Tetsuro Ogama, Ryusaburo Furuichi, and Shinichi Kikkawa

**Department of Materials Science and Engineering, Graduate School of Engineering Hokkaido University, Kita 13 Nishi 8, Sapporo, 060-8628 Japan*

High temperature oxidation of SUS430 and SUS304 stainless steels in 16.7 kPa O_2 - 20.3 kPa H_2O- balanced N2 atmosphere at 1273 K was studied focused on the scale spalling during cooling after an isothermal oxidation. Spalling of the oxide scale during cooling occurred only for SUS304 stainless steel. The oxide scale was composed of two layers and they detached at the interface between them. The reason for the spalling could not be explained only by thermal stresses applied to the specimen during heating and cooling. A new mechanism for scale spalling was proposed based on combination of thermal stresses and thermal shock caused by a fast Martensite transformation of substrate metal.

Keywords *: high temperature oxidation, spalling of scale, Martensite transformation*

1. Introduction

When stainless steels are subjected to high temperature environment, initially chromium rich oxide film covers the steel surface and the oxidation rate decreases. However in atmospheres containing water vapor, the protective oxide film breaks and an accelerated oxidation occurs. Transition from the protective to non-protective oxidation behavior is known as "break-away".[1),2)] The occurrence of break-away causes a rapid consumption of metal substrates and the prevention of the break-away is practically important. In addition, thicker oxide films formed after break-away transition sometimes cause serious troubles in steam turbine power plant or high-pressure steam boilers: the spalled scales accumulate in the bottom of boiler tubes and plug the vapor stream or sometime cause puncture of steam tubes.[3)-9)] Many reports on the effect of water vapor on the break-away have been published but there is no established mechanism which well describes break-away.[10),11)] Further, papers on the spalling of oxide scales based on the laboratory work are limited.[3)-7)]

In the present study, two commercial stainless steels, SUS430 and SUS304 were oxidized at 1273 K in O_2 - H_2O - N_2 atmosphere and spalling of oxides was followed by thermo-gravimetry (TG). With comparing the TG curves, oxide structure, and oxide composition between both alloys, a new mechanism for oxide spalling was proposed. Results of cyclic oxidation tests confirmed the mechanism.

2. Experimental

Commercial grade SUS430 and SUS304 stainless steels were used (Table 1). The specimens were polished with SiC papers down to #500 grid in distilled water and ultrasonically degreased in acetone, and then it was kept in a silica gel desiccator for more than 86.4 ks before oxidation test. High temperature oxidation tests were carried out with an infrared furnace in 16.7 kPa O_2 - 20.3 kPa H_2O - balanced N_2 atmosphere. For isothermal oxidation test, specimens were heated with 5 K s^{-1} and kept 1273 K until the mass gain of the specimen reached to about 30 g m^{-2}, and then specimens were cooled to room temperature with a controlled pattern. For cyclic oxidation test, the specimen was re-heated to 1273 K during the cooling process and the isothermal oxidation for 3.6 ks repeated 5 times. Temperatures at which re-heating started were adjusted at 473 or 773 K. Spalling of oxide scales was evaluated with weighing the specimen with a micro-balance and structure and composition of the specimens after test were analyzed with scanning electron microscope (SEM), X-ray diffraction (XRD), and X-ray photoelectron spectroscopy (XPS).

Table 1 Composition of specimens (atomic %)

Specimen	C	Si	Mn	P	S	Ni	Cr	FE
SUS304	0.37	0.96	0.82	0.05	0.01	8.09	19.02	bal.
SUS430	0.34	0.45	0.55	0.07	0.01	0.35	17.06	bal.

3. Results and discussion

3.1 High temperature oxidation of SUS430 stainless steel

Typical mass change curve of SUS430 stainless steel during the oxidation test is shown in Fig. 1. Mass of the specimen decreases steeply after the start of experiment due to a shearing force applied to the specimen by gas stream. The mass then increases parabolically with test time, ttest, indicating that a compact oxide film formed on the specimen and the oxidation rate is controlled by ion diffusion through the film. A fast oxidation occurred around t_{test}=2 ks may be due to breakdown of the oxide scales. The isothermal oxidation was terminated at t_{test}=3.48 ks at which the mass change, ΔW, reached to ΔW =21.5 g m^{-2}, and then the specimen was cooled stepwise following a temperature change curve shown in the fig. The mass increases gradually after t_{test}=3.48 ks due to a successive oxidation. No mass loss is observed for this alloy and the oxide film kept attached after the test.

More than ten runs were carried out for SUS430 stainless steel specimen terminating isothermal oxidation at heating period, t_{heat}=3.37 - 7.86 ks where mass gains at the termination, ΔW (t_{heat})=17.07-67.14 g m^{-2}, and the results are summarized in table 2. It was found that no mass loss due to spalling of the oxide scale occurs for SUS430 stainless steel independent of t_{heat} and ΔW (t_{heat}).

A cross sectional micrograph and a result of EPMA analysis for Run 7 in table 2 are shown in Fig. 2. Regions A and D in the micrograph correspond to Ni plating and alloy substrate, and the regions B and C are outer and inner oxide scales. The outer scale B is supposed to be composed of iron and oxygen. The XRD result showed

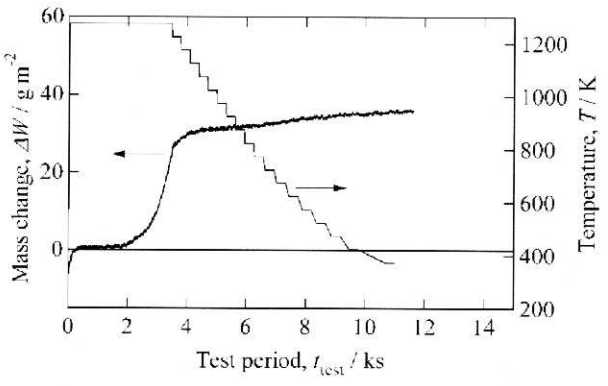

Fig. 1. Relation between mass change of SUS430 stainless steel, ΔW, and test period, t_{test}, during high temperature oxidation test in 16.7 kPa O_2 - 20.3 kPa H_2O- balanced N_2. Change in the specimen temperature is also shown.

Table 2. Summary of the oxidation tests for SUS430 stainless steels oxidized isothermally in 16.7 kPa O_2 - 20.3kPa H_2O balanced N2 atmosphere at T_{ox} = 1273K and then cooled to the room temperature stepwise.

Run	t_{heat} / ks	$\Delta W(t_{heat})$ / gm^{-2}	T_{spall} / K
1	7.86	67.14	-
2	5.23	50.36	-
3	3.37	33.73	-
4	5.40	17.07	-
5	7.20	24.17	-
6	5.40	22.59	-
7	3.48	24.17	-
8	3.72	25.69	-
9	4.02	24.36	-
10	4.20	45.45	-
11	4.80	23.01	-
Average	4.97	32.52	-
St Dev.	1.47	15.38	-

*t_{heat} is heating period, $\Delta W(t_{heat})$ mass changes at the end of isothermal oxidation, and Tspall the temperature at which the mass loss due to spalling of the oxide scale initiates.

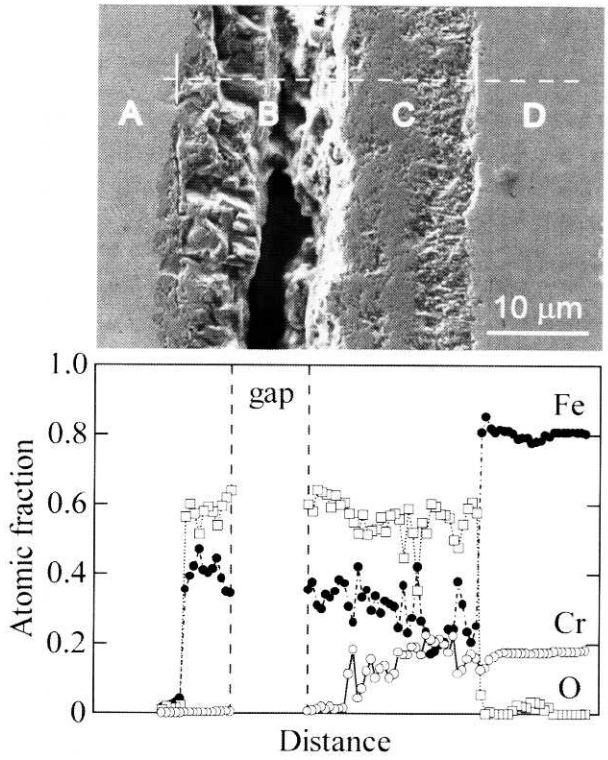

Fig. 2. A cross section and result of EPMA analysis of SUS430 stainless steel oxidized at T_{ox} = 1273 K for t_{heat} = 3.48 ks, and then cooled stepwise to room temperature (Run 7 in Table 2). Broken line in the picture is the analyzed portion, region A is Ni plating for observation, B an outer oxide scale, C an inner scale, and D substrate alloy.

this layer to be a mixture of α-Fe_2O_3 and spinel phase Fe_3O_4. Iron and chromium are detected from inner oxide scale, region C, and XRD analysis showed this scale to be a spinel phase $(Fe)(Fe,Cr)_2O_4$, in which elements in the first bracket are divalent and the rests trivalent. A sharp decrease in chromium content is observed in the alloy substrate, D, near the oxide/alloy interface and an increase in iron compensates the depletion of chromium here. This is caused by the selective oxidation of chromium: the ratio of amounts of chromium to iron in the oxide layers is calculated to be larger than that in the alloy substrate. A gap is observed in layer B that might form in the specimen preparation processes for the observation and analysis. Adhesion within the oxides in this layer may not be strong even the layers kept contacted during oxidation tests.

3.2 High temperature oxidation of SUS304 stainless steel

Mass of the specimen increases parabolically with the test period for this specimen and then an accelerated mass increase is observed (Fig. 3). The mass keeps constant after the termination of the isothermal oxidation before the specimen temperature decreases to $T = 601$ K. These behaviors are similar to that of SUS430 stainless steel shown in Fig. 1. However after the temperature of the specimen reached to $T = 601$ K, a sharp decrease in the mass. Small patches of the oxide scales were observed in the bottom of the testing tube and a sharp decrease in the mass is estimated to be due to spalling of the oxide scale. Subsequent scale spalling is observed when the specimen temperature decreased further.

To ascertain the spalling of the scales do occur for SUS304 stainless steel, oxidation tests were carried out 10 times and the results of the tests are summarized in table 3. It is evident that the spalling of the oxide scales reproduces. It should be noted that spalling temperature, T_{spall}, concentrates at 573 K with standard deviation of 23 K, in turn, the spalling occurs at almost the same tem-

Table 3. Summary of the oxidation test of SUS304 stainless steel. Oxidation condition and the annotation in the table are the same as in table 2.

Run	t_{heat} / ks	$\Delta W(t_{hest})$ / gm^{-2}	T_{spall} / K
1	3.42	24.15	573
2	4.80	24.78	579
3	3.60	25.85	534
4	4.20	14.34	597
5	2.40	20.60	598
6	4.32	24.05	546
7	4.80	20.43	601
8	4.32	24.74	598
9	3.72	22.65	578
10	7.80	20.38	577
Average	4.34	22.20	578
St Dev.	1.41	3.41	23

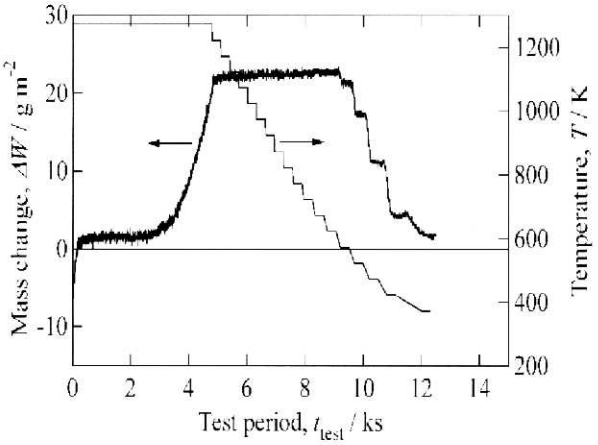

Fig. 3. Relation between mass change and temperature of SUS304 stainless steel during the test. Oxidation condition is the same as that described in Fig. 1

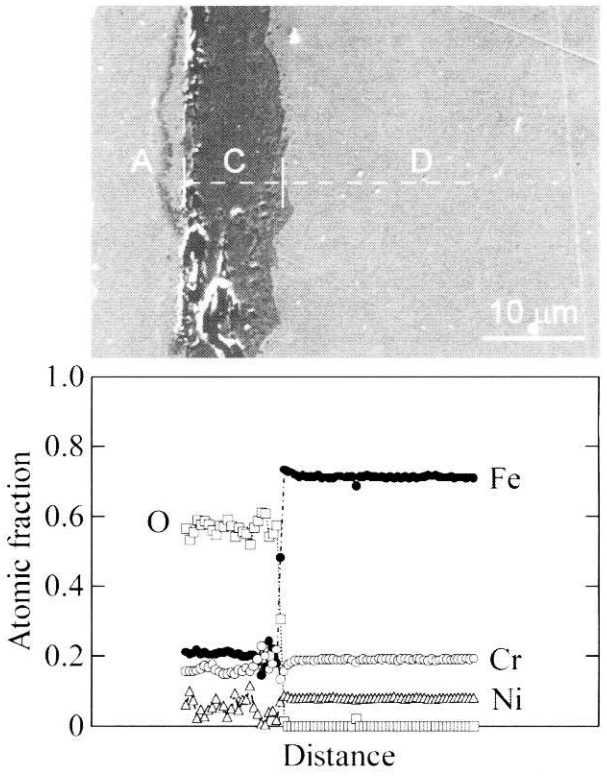

Fig. 4. Cross section and a result of EPMA analysis. The annotation in the picture is the same as that described in Fig. 2.

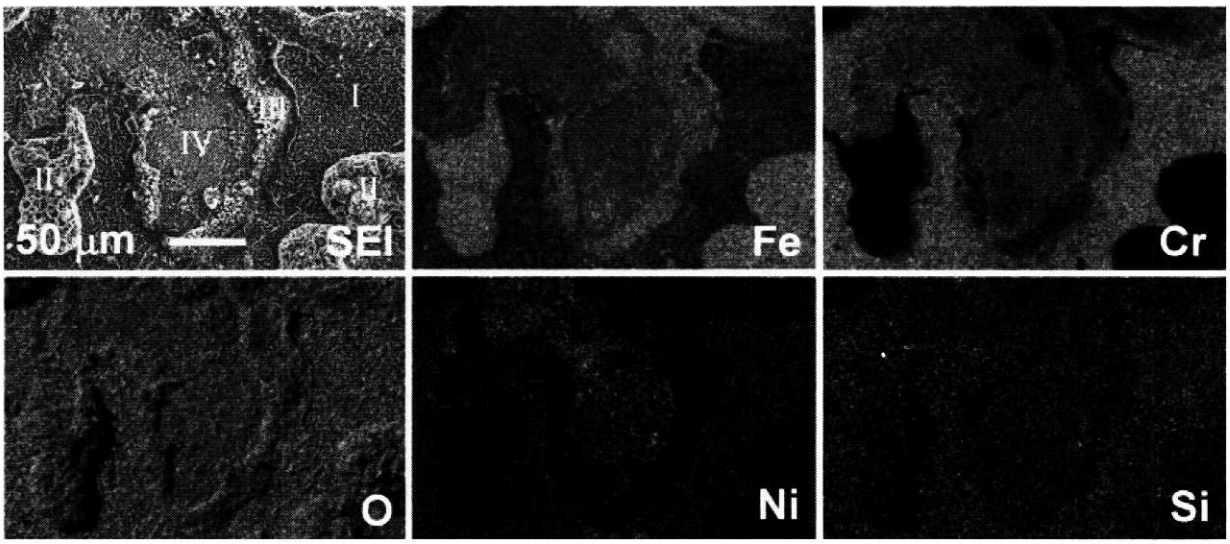

Fig. 5. Surface appearance and secondary X ray images of SUS304 stainless steel oxidized at 1273 K for 3.6 ks, and then cooled stepwise to room temperature (Run3 in table 3).

peratures for SUS304 stainless steel during cooling.

A cross section and the result of EPMA analysis for SUS304 stainless steel after the test are shown in Fig. 5. The EPMA and XRD analyses for area C showed that this oxide is composed of spinel type $(Ni,Fe)(Fe,Ni,Cr)_2O_4$. Spalled oxides are ascribed to α-Fe_2O_3 and Fe_3O_4 by XRD analysis and the thickness of spalled and remaining oxides were the same (not shown) indicating that the structure and the composition of spalled scale are the same as the outer scaled shown in Fig. 2.

A secondary electron image and X-ray images of SUS304 stainless steel surface after the oxidation test ($\Delta W(t_{heat}) = 25.85$ g m^{-2}) is shown in Fig. 5. The oxide scale can be divided to four portions. In the portion I, Cr is rich and Ni is also detected. The surface is seen to be flatter than other portions. Type II oxides are nodular and they distribute non-uniformly on the specimen surface. This oxide is composed mainly of Fe. The oxide formed at portion IV contains Fe, Cr, and Ni. Morphology and the composition of the oxide at portion III is the same as that at portion II. Comparing these results with cross sectional analysis in Figs. 2 and 4, oxide in portion II may correspond to the outer oxide scale composed of Fe_2O_3 and Fe_3O_4. The oxide in portion IV is estimated to the inner oxide scale composed of $(Ni,Fe)(Fe,Ni,Cr)_2O_4$. The portion IV was observed after spalling of the outer oxide scale occurred and the portion III is the outer oxide scale. In summary, Cr rich protective oxide film remained even after the initiation of an accelerated oxidation. Nodular oxide in portion II to IV appeared and grew at random on the surface during the accelerated oxidation, and a part of them spell during cooling.

3.3 Effect of stresses due to thermal expansion on the spalling of oxide scales

It is interesting that the spalling of the oxide scales during cooling occurred only for SUS304 stainless steel and the temperature at which the spalling start is fairly reproducible. One reason for the spalling may be the thermal stresses applied to the interface between outer and inner oxide layers due to the difference in thermal expansion coefficients between oxides.[12),13)]

Papers on the oxidation of steels and alloys in pressurized steam pointed out that difference in thermal expansion coefficients between oxide scales and substrate metals play an important roll on adherence of oxide scales.[7),8)] In this study, difference in the coefficients may also give rise to a sharing force at the interface on cooling leading to detachment of oxide scales. Effect of stresses on spalling of oxide scales should be examined based on the difference of thermal expansion coefficients of these components in table 4. Here, thermal expansion coefficients of spinel type oxides show a variation and the next discussion is divided into three according to the value of the thermal coefficient of spinel type oxides.

(1) If the thermal expansion coefficients of spinel type oxide is assumed to about 10, the smallest choice, good adherence between oxide and substrate for SUS430 stainless steel is expected and the stress may be applied at the interface between spinel oxide layer and substrate metal for SUS304 stainless steel. In this case reason why spalling occur at the interface between outer and inner

Table 4 Thermal expansion coefficientof oxides and stainless steels.

Substance	TEC $\times 10^6/K^{-1}$	Temperature/K	ref.
Fe_2O_3	10.96(298K)-14.13(1273K)	298-1273	12
Fe_3O_4	10(273K)-28(823K)	273-873	12
$(Fe, Cr)_3O_4$	10(273K)-28(823K)	273-873	12
$NiCr_2O_4$	10	298-1473	12
SUS430	10.2(373K)-12.3(1150K)	373-1150	13
SUS304	17.7(373K)-20.5(1073K)	373-1073	13

* TEC : theral expansion coefficient

oxide layers can not be explained.

(2) Assuming that the thermal expansion coefficient of spinel type oxide layer as about 28, the largest choice, stress may be applied at all interfaces for both alloys. The largest stress will be generated at the interface between oxide and substrate for SUS430 stainless steel and it is hard to explain the experimental results.

(3) If the thermal expansion coefficient of spinel type oxide is assumed to be around 17, good adherence between oxide and substrate for SUS304 stainless steel is expected. With this assumption, spalling of the scale will be occur for SUS430 stainless steel but the assumption did not match experimental results.

The assumption (1) could stand if the spinel type oxides are assumed to deform during cooling and thermal expansion coefficients apparently match that of substrate metals. Provided that spinel type oxide deforms elastically and a simple Fook's raw can be applied to the oxide, the thinner the oxide layers the smaller sharing force at the interface of both layers. However, the temperatures at which the spalling took place do not depend on $\Delta W(t_{heat})$. If the outer oxide layer can deform plastically, an accumulation of sharing force at the interface will be released resulting a prevention of spalling. The required stress for plastic deformation should be large for thicker oxide layer but the experimental result did not show any increase in T_{spall}, with $\Delta W(t_{heat})$.

In summary, spalling of outer oxide layer formed on SUS304 stainless steel cannot be explained only by considering the thermal stresses generated on cooling.

3.4 Effect of thermal shock by Martensite transformation as a reason of scale spalling

It is notable that standard deviation of T_{spall} of SUS304 stainless steel is small as 23 K and the temperatures is seemed to reproducible even the spalling occurred random at the surface. Some papers that cover the spalling of outer oxide layer formed on steels and alloys report that there is a critical thickness above which the spalling takes

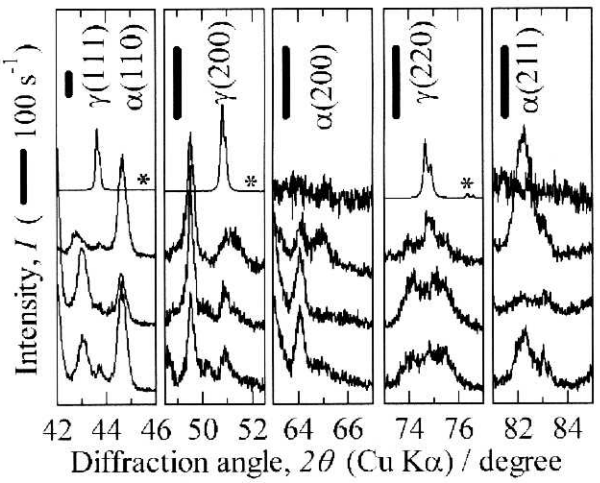

Fig. 6. The X-ray diffraction patterns of SUS304 stainless steels. Curve (1) was taken before oxidation test and (2), (3), and (4) were taken after the test and correspond to Run 2, 3, and 7 in table 3. Curves with a mark (*) are compressed 1/100 with Y-axis.

place.[6),7)] Another study of authors varying $\Delta W(t_{heat})$ from 5 to 100 g m^{-2} showed no mass gain dependence of spalling as in the present study indicating that there is no critical thickness for the spalling in O_2 - H_2O containing atmosphere or that the mechanism of spalling is different with that observed for steam oxidation.

Fig. 7 shows XRD patterns of SUS304 stainless steel before and after the oxidation tests. Diffraction peaks of α-iron are observed for all SUS304 specimens after oxidation test that are not detected for the specimen after a slight annealing in Argon atmosphere. Selective oxidation of chromium forms a chromium deficient zone in the outermost of the substrate metal (Fig. 4). This causes a stabilization of γ-phase at 1273 and the α-phase cannot form. Transformation from γ to α (Martensite) can take place for austenitic stainless steels and the transition temperature, *Ms*, is reported to follow equation 1.[13)]

$$Ms = 1305 - 41.7[\%Cr] - 61[\%Ni] - 33[\%Mn] - 27.8[\%Si] - 1667[\%C + \%N] \quad (1)$$

here, variables in blackest and Ms are represented by mass % and in K.

As shown in Fig. 4, Cr content in the substrate drops steeply toward the interface between oxide and substrate, and Fe compensate the deficient of Cr. No accumulation of Ni is observed there that may be due to back diffusion of Ni to the substrate. Assuming that *Ms* = 601 K and the contents of element other than Cr near the interface do not change during oxidation test, equation 1 gives [%*Cr*]

= 0.48 (0.51 atomic%). Concentration drop of Cr to 0.51 at% near the interface was not detected in Fig. 4 within the spatial resolution of EPMA but the drop can occur in principle.[14] Therefore the α phase observed in Fig. 6 can be explained reasonably by γ to α (Martensite) transformation.

Velocity of Martensite transformation is reported to fast[13] and it can give a shock to the specimen. Because the occurrence of Martensite transformation is limited to SUS304 stainless steel, the shock due to the transformation can be the reason why the spalling occurred only for SUS304 stainless steel. Any thermal stress is also required to the spalling and it can be supposed that the stress concentrated at the interface between outer and inner oxide layers.

3.5 Cyclic oxidation test

In the previous sections, a probable model of the scale spalling during cooling has been proposed to the release of thermal stress triggered by γ to α (Martensite) transformation of the substrate. If these assumption is valid, the spalling is expected to avoid by keeping the specimen temperature above *Ms*. To proof this assumption, a cyclic oxidation test was carried out.

Mass changes during cyclic oxidation tests are shown in Fig. 7. Minimum temperatures during the cycles are adjusted to (a) 473 and (b) 773 K. When the cyclic oxidation test is switched at 473 K, mass loss is observed during cooling after the first isothermal test and the onset temperature of the mass loss is estimated to 673 K. This temperature is in the range of temperatures in table 2 at which the spalling started. While the cyclic test was carried out between 773-1273 K, essentially no mass loss is observed in spite of the cooling after cycling test.

Cross sections of the specimens after the cyclic oxidation are shown in Figs. 9 and 10. Most of the surface is covered with two layered oxides similar to what shown in Fig. 2 indicating that no spalling was occurred during cyclic oxidation test except final cooling to the room temperature when the cyclic oxidation test repeated at 773 K (Fig. 8). On the other hand, the oxides formed when the test repeated in 1273 - 473 K (Fig. 9) the thickness

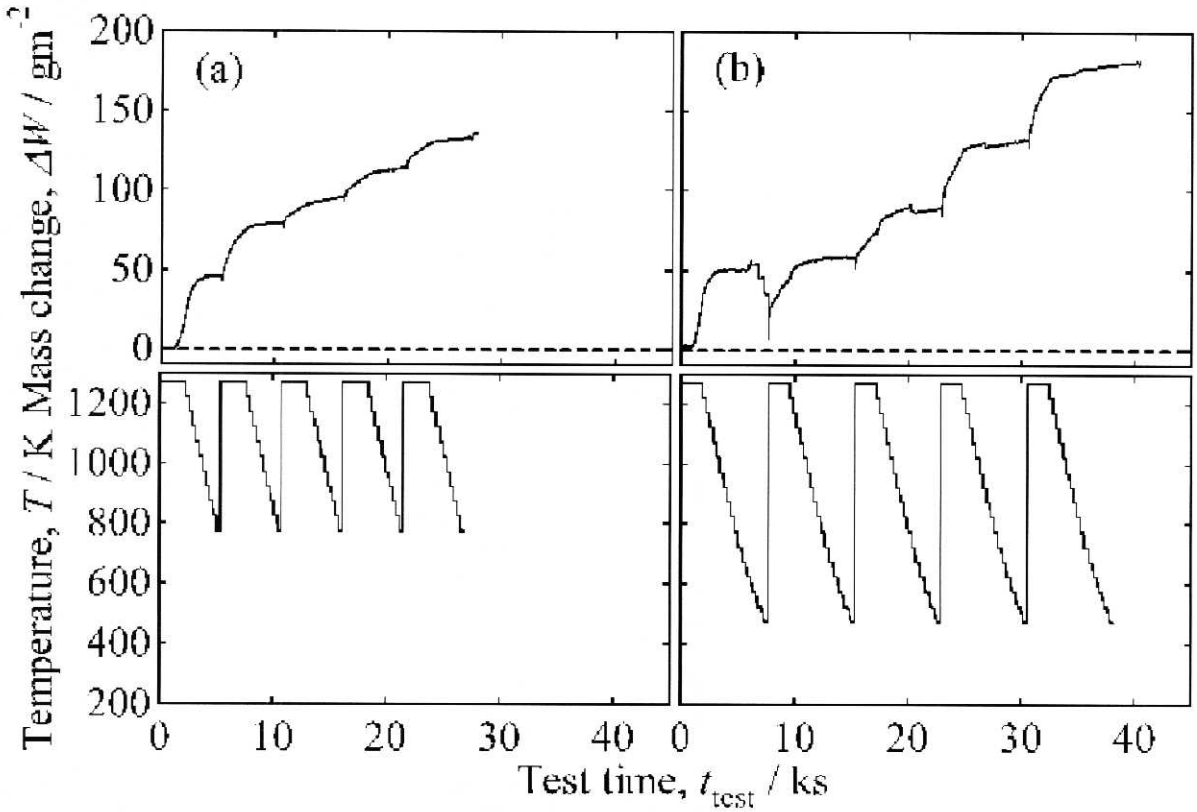

Fig. 7. Changes in mass and the temperature of SUS304 stainless steel during a cyclic oxidation test in 16.7 kPa O_2 - 20.3 kPa H_2O- balanced N_2 atmosphere. The isothermal oxidation at 1273 K continues 3.6 ks and the cycle repeated while the temperature of the specimen decreased at (a) 773 K and (b) 473 K.

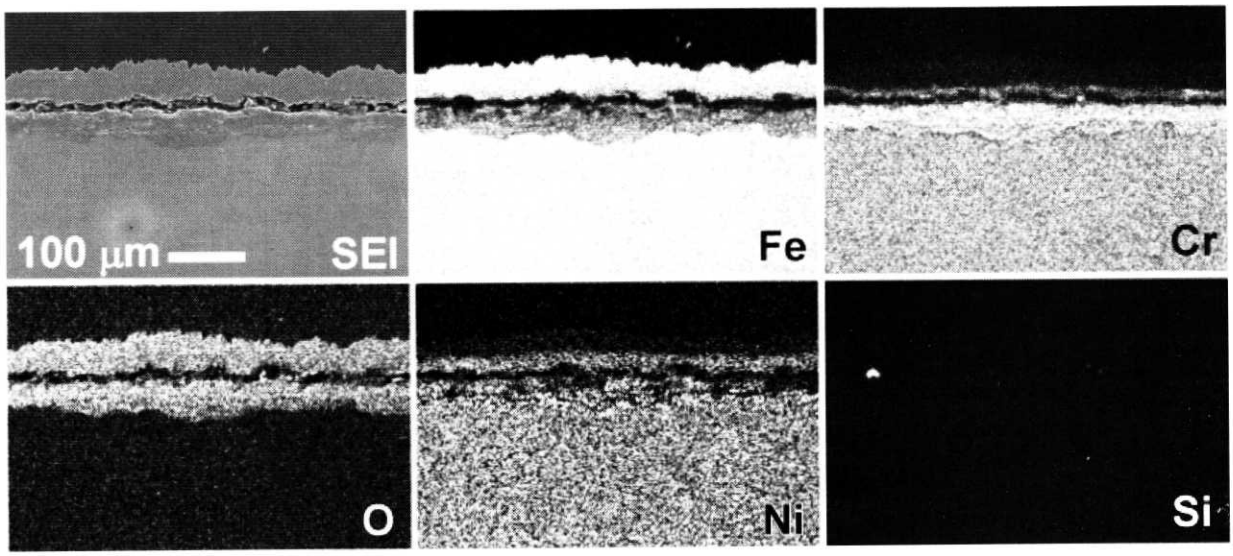

Fig. 8. Secondary electron image and X ray images of the cross section for SUS304 stainless steel after a cyclic oxidation test shown in Fig. 7.

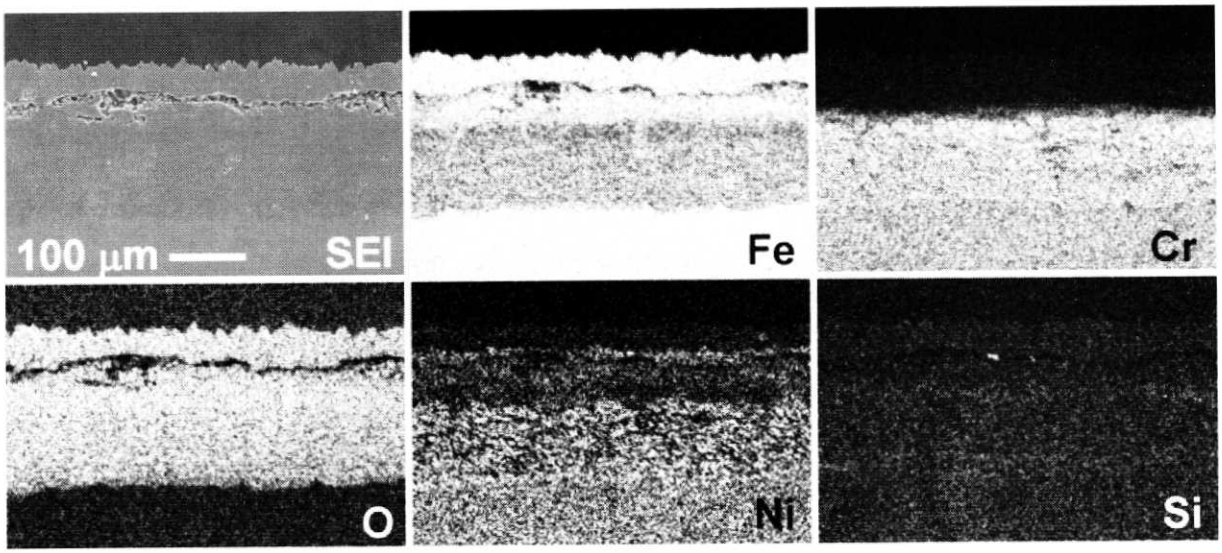

Fig. 9. Secondary electron image and X ray images of the cross section for SUS304 stainless steel after a cyclic oxidation test shown in Fig. 7.

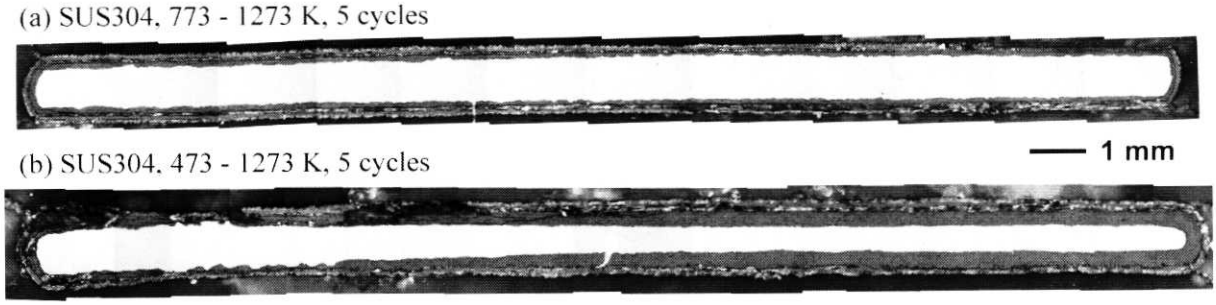

Fig. 10. Low magnification pictures of cross sections of SUS304 stainless steels after cyclic oxidation test detailed in Fig. 7.

of the inner oxide layer is far thicker than that shown in Fig 8.

Fig. 10 shows cross section of specimens after cyclic oxidation. It is clear that remaining metal substrate in Fig. 10(a) is a fourth of that in Fig. 10(b). These results indicate that once the oxide scale spalled the protective properties ox the scales disappear. In turn, the outer oxide layer formed in the initial isothermal oxidation periods is so effective to prevent fast oxidation of SUS304 stainless steel at high temperatures.

4. Conclusions

High temperature oxidation tests of SUS430 and SUS304 stainless steels were carried out in 16.7 kPa O_2 - 20.3 kPa H_2O- balanced N_2 atmosphere at 1273 K and the following conclusions are obtained.

(1) Spalling of the oxide scales during cooling occurs only for SUS304 stainless steel. The oxide detached at the interface between outer and inner oxide layers. The reason for the spalling is estimated to be a sudden release of accumulated stress at the interface during cooling triggered by a fast volume change through Austenite to Martensite transformation of alloy phase.

(2) If the alloy temperature is kept higher than the transformation temperature to Martensite phase (Ms) the spalling can avoid, or serious oxidation of SUS304 stainless steel takes place. In the latter case increase in the thickness of inner oxide scale is evident and it indicates the outer oxide scale composed of Fe_2O_3 and Fe_3O_4 is much resistant to oxidation at high temperature than inner oxide scale.

Acknowledgements

A part of this study is supported by Grant-in-aid for Scientific Research of Ministry of Education, Science, and Sports, Japan (12650705), KAWASAKI STEEL 21st Century Foundation, and foundation for study on steels ISIJ.

References

1. P. Kofstad, *High Temperature Corrosion*, Elsevier, 1988, p. 258.
2. G. C. Wood and D. P. Whittle, *Corros. Sci*, **4**, 293 (1964).
3. G. P. Wozaldo and W. L. Pearl, *Corrosion*, **21**, 355 (1965).
4. T. Ericsson, *Oxid. Metals*, **2**, 173 (1970).
5. H. Usuda, Y. Sakumoto, Y. Harada, and U. Akita, *Mitsubishi Heavy Ind. Tech. Rev.*, **8**, 649 (1971) *in Japanese.*
6. T. Moroishi, *Tech. Rep. Sumitomo Metal Ind.*, **25**, 117 (1973) *in Japanese.*
7. K. Suzuki, O. Asai, H. Iwata, and T. Kanbayashi, *Karyoku-Gennshiryoku-Hatsuden*, **27**, 27 (1976) *in Japanese.*
8. D. L. Deadmore and C. E. Lowell, *Oxid. Metals*, **11**, .91 (1977).
9. H. E. Evans, *Matl. Sci. Tech.*, **4**, 415 (1988).
10. C. T. Fujii, and R. A. Meussner, *J. Electrochem. Soc.*, **111**, 1215 (1964).
11. K. Nii, *Bousyoku-Gizyutsu*, **26**, 389 (1977) *in Japanese*
12. M. Schuetze, *Protective Oxide Scales and Their Breakdown*, Wiley, 1997.
13. Stainless steel society of Japan, *Stainless Steel Handbook, 3rd ed.*, Nikkan Kogyo Shinbun, 1995, p.77, 1427 *in Japanese.*
14. C. Wagner, *J. Electrochem. Soc.*, **99**, 369 (1952).